CD300f immunoreceptor is associated with major depressive disorder and decreased microglial metabolic fitness

Natalia Lago[a,1], Fernanda N. Kaufmann[b,1], María Luciana Negro-Demontel[a,c], Daniela Alí-Ruiz[a], Gabriele Ghisleni[d], Natalia Rego[e], Andrea Arcas-García[f], Nathalia Vitureira[a,g], Karen Jansen[d], Luciano M. Souza[d], Ricardo A. Silva[d], Diogo R. Lara[h], Bruno Pannunzio[a,c], Juan Andrés Abin-Carriquiry[i], Jesús Amo-Aparicio[j], Celia Martin-Otal[f], Hugo Naya[f], Dorian B. McGavern[k], Joan Sayós[f], Rubèn López-Vales[j], Manuella P. Kaster[b], and Hugo Peluffo[a,c,2]

[a]Neuroinflammation and Gene Therapy Laboratory, Institut Pasteur de Montevideo, 11400 Montevideo, Uruguay; [b]Department of Biochemistry, Federal University of Santa Catarina, Florianópolis, 88040-900 Santa Catarina, Brazil; [c]Departamento de Histología y Embriología, Facultad de Medicina, Universidad de la República, 11200 Montevideo, Uruguay; [d]Department of Life and Health Sciences, Catholic University of Pelotas, 96015-560 Rio Grande do Sul, Brazil; [e]Bioinformatics Unit, Institut Pasteur de Montevideo, 11400 Montevideo, Uruguay; [f]Immune Regulation and Immunotherapy Group, CIBBIM-Nanomedicine, Vall d'Hebrón Institut de Recerca, Universitat Autònoma de Barcelona, 08193 Barcelona, Spain; [g]Department of Physiology, Facultad de Medicina, Universidad de la República, 11200 Montevideo, Uruguay; [h]Department of Cellular and Molecular Biology, Pontifical Catholic University of Rio Grande do Sul, 90619-900 Porto Alegre, Brazil; [i]Instituto de Investigaciones Biológicas Clemente Estable, 11600 Montevideo, Uruguay; [j]Departament de Biologia Cel·lular, Fisiologia i Immunologia, Institut de Neurociències, Centro de Investigación Biomédica en Red sobre Enfermedades Neurodegenerativas, Universitat Autònoma de Barcelona, 08193 Bellaterra, Spain; and [k]Viral Immunology and Intravital Imaging Section, National Institute for Neurological Disorders and Stroke, National Institutes of Health, Bethesda, MD 20892

Edited by Shizuo Akira, Osaka University, Osaka, Japan, and approved February 4, 2020 (received for review July 11, 2019)

A role for microglia in neuropsychiatric diseases, including major depressive disorder (MDD), has been postulated. Regulation of microglial phenotype by immune receptors has become a central topic in many neurological conditions. We explored preclinical and clinical evidence for the role of the CD300f immune receptor in the fine regulation of microglial phenotype and its contribution to MDD. We found that a prevalent nonsynonymous single-nucleotide polymorphism (C/T, rs2034310) of the human CD300f receptor cytoplasmic tail inhibits the protein kinase C phosphorylation of a threonine and is associated with protection against MDD, mainly in women. Interestingly, CD300f$^{-/-}$ mice displayed several characteristic MDD traits such as augmented microglial numbers, increased interleukin 6 and interleukin 1 receptor antagonist messenger RNA, alterations in synaptic strength, and noradrenaline-dependent and persistent depressive-like and anhedonic behaviors in females. This behavioral phenotype could be potentiated inducing the lipopolysaccharide depression model. RNA sequencing and biochemical studies revealed an association with impaired microglial metabolic fitness. In conclusion, we report a clear association that links the function of the CD300f immune receptor with MDD in humans, depressive-like and anhedonic behaviors in female mice, and altered microglial metabolic reprogramming.

microglia | RNA-seq | depression | immunereceptor | CD300

Under physiological conditions, microglial cells continuously sense the neural environment and rapidly respond to neuronal activity, capillary leakage, cellular debris, and pathogens. Altered microglial function was postulated to contribute to psychiatric diseases including major depressive disorder (MDD) (1, 2). A significant association was observed between microglial and perivascular macrophage activation or increased cell number and untreated long-term MDD, as evidenced by brain translocator protein 18 kDa (TSPO) PET ligand [18F]FEPPA staining (2). Interestingly, antidepressant treatment prevented the progressive TSPO staining and MDD symptoms (2). The chronic microglial dysfunction associated with a dystrophic phenotype and increased cell numbers observed in MDD is accompanied by a well-documented increase in serum levels of inflammatory cytokines including interleukin 1 receptor antagonist (Il1rn) and interleukin 6 (IL-6) (3, 4). Despite the rapid advance in massive sequencing capacities, no microglial-specific transcriptomic profile has been published for the major psychiatric disorders. Very recently, transcriptomic methods have contributed to the precise description of a microglial phenotype termed disease- or damage-associated microglia (DAM) (5, 6). An interesting emerging hypothesis postulates that under neurodegenerative conditions or aging (6–8), the down-regulation of this homeostatic phenotype may impact central nervous system (CNS) dysfunction per se (9). It is therefore interesting to determine if this microglial phenotype is associated with psychiatric diseases.

Activating and inhibitory immunoreceptors, signaling mainly through DAP12 (also known as TYROBP) (8), were shown to

Significance

A role for innate immune receptors expressed by microglia and barrier macrophages has been postulated in neuropsychiatric diseases, including major depressive disorder (MDD). We discovered that a prevalent single-nucleotide polymorphism of the human CD300f immune receptor alters its signaling and is associated with protection against MDD in women but not in men. Interestingly, CD300f-deficient female, but not male, mice displayed depressive-like behaviors. In these mice, the absence of CD300f induced phenotypical changes of microglial cells that altered their metabolic fitness. Despite the high incidence of MDD, no effective treatments are available in many cases, and these discoveries could lead to the development of new pipelines for drugs targeting microglial cells, perivascular macrophages, and in particular the CD300f immune receptor.

Author contributions: N.L., F.N.K., G.G., N.R., N.V., J.A.-A., H.N., D.B.M., J.S., R.L.-V., M.P.K., and H.P. designed research; N.L., F.N.K., M.L.N.-D., D.A.-R., G.G., N.R., A.A.-G., N.V., K.J., L.M.S., R.A.S., D.R.L., B.P., J.A.A.-C., J.A.-A., C.M.-O., J.S., M.P.K., and H.P. performed research; N.L., M.L.N.-D., N.R., N.V., H.N., D.B.M., J.S., and R.L.-V. contributed new reagents/analytic tools; N.L., F.N.K., M.L.N.-D., D.A.-R., G.G., N.R., A.A.-G., N.V., J.A.-A., H.N., J.S., R.L.-V., M.P.K., and H.P. analyzed data; and N.L., F.N.K., N.R., M.P.K., and H.P. wrote the paper.

The authors declare no competing interest.

This article is a PNAS Direct Submission.

Data deposition: Raw data from the RNA sequencing experiment have been deposited in the NCBI Sequence Read Archive, https://www.ncbi.nlm.nih.gov/sra (accession no. PRJNA496060).

[1]N.L and F.N.K. contributed equally to this work.

[2]To whom correspondence may be addressed. Email: hugo.peluffo@pasteur.edu.uy.

This article contains supporting information online at https://www.pnas.org/lookup/suppl/doi:10.1073/pnas.1911816117/-/DCSupplemental.

First published March 9, 2020.

play a central role in microglial function both in the healthy and lesioned nervous system (5, 8, 10, 11). In particular, inhibitory immune receptors act as microglial restraining signals or checkpoints, ensuring mechanisms that actively limit microglial reactivity under both physiological and pathological conditions (12, 13). Activating and inhibitory immune receptors in microglial cells, such as TREM2, participate in synaptic pruning and clearance of cellular debris and apoptotic cells in the CNS (14). Although no microglial immune receptors have been associated to human MDD, a deficiency in the microglial immune receptors TREM2 or CX3CR1 induce alterations in social interaction and compulsive behaviors in naïve mice (14, 15) or potentiate depressive-like behaviors induced by lipopolysaccharide (LPS) (16), highlighting their putative role in psychiatric conditions.

Despite the importance of immune receptors on microglial function, many of them have not been studied in detail. In particular, CD300f immune receptors, which are expressed by several CNS myeloid cells including microglia and perivascular macrophages (5), share common phospholipid ligands with TREM2 such as the eat-me signal phosphatidylserine (17, 18), sphingomyelin (19), and high-density lipoprotein (HDL) and low-density lipoprotein (LDL) (20) and indirectly modulate DAP12 (21). CD300f is a very unique receptor, as it displays a dual activating/inhibitory capacity, recruiting phosphatases like SHP1/SHP2 via its ITIM motifs as well as activating PI3K and Grb2 adaptors, among others (22, 23). Moreover, it directly modulates other receptors, such as several members of the CD300 receptor family including CD300b activating receptor (21), FcRγ (24), and IL4Rα (25). In accordance with its inhibitory function, the absence of CD300f potentiates many inflammatory/autoimmune disease models (20, 26, 27) and is associated with human inflammatory and autoimmune disease susceptibility (28, 29).

Regardless of the strong evidence suggesting the importance of this receptor for the regulation of inflammatory conditions, very few studies have evaluated its role in the nervous system. CD300f is particularly interesting for the CNS demyelinating diseases, as it was shown to play a key role in experimental autoimmune encephalomyelitis, where exacerbated neuroinflammatory pathology is found in the knockout animals (30), and also being among the genes up-regulated in promyelinating microglia after a demyelinating stimuli (31). It appears among the top up-regulated genes in brain microglia after intraperitoneal (i.p.) LPS injection (32) and after spinal cord injury (33). Very recently, it was also associated to the neuroprotective response against Tau pathology (34). Despite all of this evidence implicating CD300f in CNS physiology and pathophysiology, no one has revealed any behavioral phenotypes in CD300f$^{-/-}$ mice under naïve conditions (20, 30, 35), and no studies have been performed in the CNS of these animals.

Here, we explored the participation of the CD300f immune receptor in regulating neuroinflammation as well as its involvement in behavioral alterations in mice and humans relevant for MDD.

Results

Association of a CD300f SNP with MDD. A single-nucleotide polymorphism (SNP, rs2034310) in the CD300f immune receptor has been associated with multiple sclerosis (29). This genetic variation is highly prevalent and determines a C/T exchange (mean frequencies ∼18 and 29% of European and American populations, respectively), producing a nonsynonymous substitution from Arg to Gln (R218Q) in the intracellular tail of CD300f. We took advantage of this natural highly prevalent polymorphism to evaluate its possible association with MDD in a cross-sectional population-based study. The study comprised a total of 1,110 individuals, 625 controls without MDD and 485 with MDD diagnosis. The sociodemographic information according to diagnosis is depicted in *SI Appendix*, Table S1. A high prevalence of MDD was observed in women ($P < 0.001$) and between smokers ($P < 0.001$). When analyzing the sociodemographic variables according to genotype distribution, we did not find differences according to sex ($P = 0.860$), socioeconomic class ($P = 0.964$), body mass index ($P = 0.524$), or presence of inflammatory or metabolic diseases ($P = 0.697$). However, ethnicity was significantly associated to genotype and the presence of the T allele was significantly higher in non-Caucasian individuals ($P < 0.001$). Additionally, the genotype frequencies were in agreement with those predicted by Hardy–Weinberg equilibrium for the rs2034310 SNP ($\chi^2 = 0.043$, $P = 0.836$). When evaluating the genotype frequencies according to diagnosis (*SI Appendix*, Table S2), it was observed that the CT genotype was associated with a protection against MDD when compared to the CC genotype (odds ratio [OR] = 0.693 95% CI 0.538 to 0.891; $P = 0.004$). This association remained significant after adjusting for age, sex, and ethnicity (OR = 0.698 95% CI 0.539 to 0.903; $P = 0.006$). Due to the small number of individuals with the TT genotype, we further used the dominant model grouping CT and TT subjects. The presence of the T allele (CT/TT) also conferred protection against MDD when compared to the CC genotype (OR = 0.736 95% CI 0.578 to 0.937; $P = 0.013$). These effects remained independently associated with protection against MDD after adjustment for the same variables described above (OR = 0.740 95%CI 0.578 to 0.948; $P = 0.017$), suggesting that genetic alterations in CD300f receptor function may impact susceptibility to MDD. Additionally, no significant allelic distribution differences were observed between C and T carriers according to MDD diagnosis ($P = 0.110$). An important point that has been neglected in psychiatric research is the evaluation of biological mechanisms underlying sex differences. In fact, MDD is twofold more prevalent in women and the lack of sex-specific biological evaluations can partially explain the treatment resistance and relapse for this disorder. To unravel possible sex-specific associations between the CD300f SNP and MDD, we stratified our sample (Table 1) and found that the association of the T allele with protection against MDD was only observed in women (OR = 0.625 95%CI 0.454 to 0.861; $P = 0.004$), even after adjusting for possible confounders (OR = 0.632 95% CI 0.457 to 0.874; $P = 0.006$). Despite the lower power of analysis obtained in the stratified sample of men (52.24%) when compared to the women's sample (99.59%), these results might suggest that sex differences might account for the influence of CD300f receptors on MDD.

Peripheral NLRP3/Caspase 1/IL-1β–mediated inflammation has been linked to a group of MDD patients (36); however, the CT genotype was not associated with increased serum IL-1β levels (CC: 9.66 ± 1.34 pg/mL, CT: 10.65 ± 1.47 pg/mL, and TT: 10.52 ± 4.98 pg/mL; $F(2.165) = 0.15$, $P = 0.559$). Thus, alterations in CD300f signaling may be associated with MDD in the absence of peripheral IL-1β–dependent inflammation.

The SNP Affects CD300f Immune Receptor Signaling. The arginine R218 to glutamine amino acid (R218Q) substitution in the intracellular tail of CD300f that confers protection against female depression is in the context of a putative protein kinase A (PKA)/protein kinase C (PKC) phosphorylation motif. To test this hypothesis COS7 cells transfected with human CD300f receptor (hCD300f) were submitted to different treatments: pervanadate (inhibiting phosphatases), forskolin (activating PKA), and phorbol-*myristate*-acetate (PMA) (activating PKC). Western blots using antibodies against specific phosphoSer/Thr recognizing the motif [R/K][R/K]X[pS/pT] demonstrated a PKC-dependent pS/pT phosphorylation of CD300f (Fig. 1*A*). This Ser/Thr phosphorylation was dependent on the R218 arginine residue, as the substitution of this amino acid by a glutamine blunted the phosphorylation (Fig. 1*B*). Therefore, we concluded that R218 is necessary for the PKC phosphorylation of CD300f cytoplasmic tail. Moreover, mutants of the serine S216, threonine T221, or both, demonstrated that the threonine T221 is the

Table 1. Genotype and allele distribution according to sex and diagnosis for MDD

Characteristics	MDD				
	No	Yes	*P*	Unadjusted OR (95%)/*P**	Adjusted OR (95%)/*P*†
Women					
rs2034310 SNP genotype					
CC	154 (51.2)	201 (62.6)	0.006	1	1
CT	131 (43.5)	100 (31.2)		0.585 (0.419–0.817)/0.002	0.592 (0.422–0.831)/**0.002**
TT	16 (5.3)	20 (6.2)		0.958 (0.480–1.910)/0.902	0.964 (0.481–1.935)/0.919
Dominant model					
CC	154 (51.2)	201 (62.6)	0.005	1	1
CT/TT	147 (48.8)	120 (37.4)		0.625 (0.454–0.861)/0.004	0.632 (0.457–0.874)/**0.006**
Men					
rs2034310 SNP genotype					
CC	182 (56.2)	95 (58.3)	0.626	1	1
CT	127 (39.2)	58 (35.6)		0.875 (0.588–1.302)/0.510	0.886 (0.594–1.321)/0.551
TT	15 (4.6)	10 (6.1)		1.277 (0.553–2.952)/0.567	1.307 (0.564–3.029)/0.533
Dominant model					
CC	182 (56.2)	95 (58.3)	0.657	1	1
CT/TT	142 (43.8)	68 (41.7)		0.917 (0.627–1.343)/0.657	0.929 (0.634–1.364)/0.708

Data are presented as number (percent) or proportion.
**P* values were computed by χ^2 tests comparing MDD patients and controls.
†Adjusted OR (95% CI/*P*) values were obtained from logistic regression analysis adjusting for age and ethnicity. Significance of adjusted OR is highlighted in bold.

only residue phosphorylated by PKC in the cytoplasmic tail of hCD300f (Fig. 1*C*). We also observed that the phosphorylation of T221 is an event downstream of the phosphorylation of the five tyrosine residues within the cytoplasmic tail of CD300f (*SI Appendix*, Fig. S1*A*), and also that the two tyrosine residues that conform the putative PLCγ binding motifs, Y205 and Y236, could

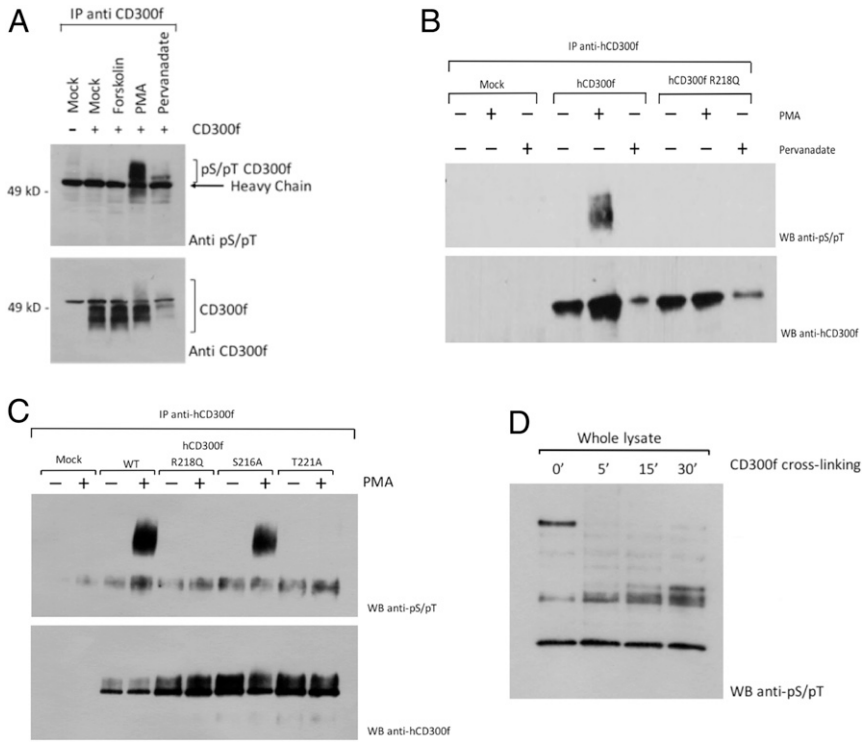

Fig. 1. The R218Q substitution of CD300f SNP modifies its normal signaling. COS-7–transfected cells with an empty vector or the hCD300f construct were exposed to different stimuli. Immunoprecipitation (IP) with anti-CD300f monoclonal antibody (mAb) was performed and Western blot with a Phospho-(Ser/Thr) PKA Substrate Antibody, which detects phospho-serine/threonine residue with arginine at the −3 position (K/R)(K/R)X(pS/pT). Blotting with anti-CD300f Ab was done as loading control (*A*). COS-7 cells were transfected with an empty vector or the indicated hCD300f constructs and cells were treated with PMA or pervanadate. IP with anti-CD300f mAb was performed and blots were performed with Phospho-(Ser/Thr) PKA Substrate Antibody. Blotting with anti-CD300f Ab was performed as loading control (*B*). COS-7 cells were transfected with an empty vector or the indicated hCD300f constructs. When indicated, transfected cells were exposed to PMA, IP with anti-CD300f mAb was performed, and blots were processed with Phospho-(Ser/Thr) PKA Substrate Antibody. Blotting with anti-CD300f Ab was performed as loading control (*C*). U937 cells were stimulated with 10 μg/mL UPD2 mAb for different periods. An IP with anti-CD300f mAb was performed and proteins were blotted with Phospho-(Ser/Thr) PKA Substrate Antibody (*D*).

be essential for the activation of PLCγ, which in turn promotes the activation of PKC (*SI Appendix*, Fig. S1 *B* and *C*). Moreover, we discovered that PKC activation is part of the normal CD300f signaling pathway using the U937 monocytic cell line (Fig. 1*D*). Collectively, these data (Fig. 1 and *SI Appendix*, Fig. S1) show that PKCδ isoenzyme is involved in the CD300f activating signaling and that the R218Q substitution of SNP modifies its normal signaling.

CD300f Deficiency Induces Depressive-Like Behavior and Anhedonia in Female Mice. The association of the rs2034310 CD300f SNP with MDD prompted us to analyze possible changes in the general behavioral phenotype of the CD300f$^{-/-}$ mice, especially behavioral alterations considered relevant for MDD. Three different strains of CD300f$^{-/-}$ mice have been generated to date, including the one used in the present study. None of these knockouts have reported alterations in development or other basic physiological variables, including immune system function or systemic inflammation in naïve conditions (20, 30, 35). However, no behavioral studies have been performed on these animals. When 4- to 5-mo-old wild-type (WT) and CD300f$^{-/-}$ mice of both sexes were exposed to an open field arena [in the parallel rod floor test arena (37)], the CD300f$^{-/-}$ animals displayed decreased spontaneous locomotor activity (Fig. 2*A*). However, these animals did not show alterations in motor coordination or ataxia when analyzed both by the parallel rod floor test (37) (Fig. 2*B*) or when exposed to a forced locomotor task such as the rotarod (Fig. 2*C*). These results suggest that CD300f$^{-/-}$ mice do not have a defect in motor function that explains the reduced spontaneous activity. The adult CD300f$^{-/-}$ female and male animals did not show other general alterations in CNS physiology such as the thermal sensitivity of the hind paws measured by the Hargreaves test (*SI Appendix*, Fig. S2*A*) or in the mechanical sensitivity of the hind paws tested with the Von Frey filaments (*SI Appendix*, Fig. S2*B*). Additionally, adult male and female mice were exposed to behavioral despair models such as the tail suspension test (TST) and the forced swim test (FST) and to the sucrose splash test (SST) to evaluate motivational and hedonic behaviors. These tests assess the two cardinal symptoms of MDD: depressive-like behavior and anhedonia (loss of pleasure seeking). Female CD300f$^{-/-}$ mice did not show significant alterations in spontaneous locomotor activity in a regular open field test (OFT) (Fig. 2*D*); however, they displayed a significant increase in immobility time when compared to WT animals in both the TST (Fig. 2*E*) and the FST (Fig. 2*F*) that reflects a depressive-like behavior. Moreover, the female CD300f$^{-/-}$ animals showed a significant decrease in the total time spent grooming after the sucrose splash when compared to WT animals (Fig. 2*G*) and an increase in the latency to start grooming, indicative of reduced motivational behavior (Fig. 2*H*). Together, these results suggest that female CD300f$^{-/-}$ mice displayed anhedonic behaviors. CD300f deficiency also potentiated the anhedonic behavior observed in the LPS-induced depression model in female mice (Fig. 2*I*), showing that the absence of this receptor may contribute to multifactorial mechanisms of depressive behaviors. Interestingly, the depressive-like and anhedonic symptoms were not observed in adult 4- to 5-mo-old males (*SI Appendix*, Fig. S3). Finally, to test whether CD300f$^{-/-}$ female mice have long-lasting and progressive MDD-like behavioral alterations, we exposed a different cohort of aged females (18 mo old) to the previous behavioral test batteries. Aged CD300f$^{-/-}$ female mice (aCD300f$^{-/-}$) had an altered

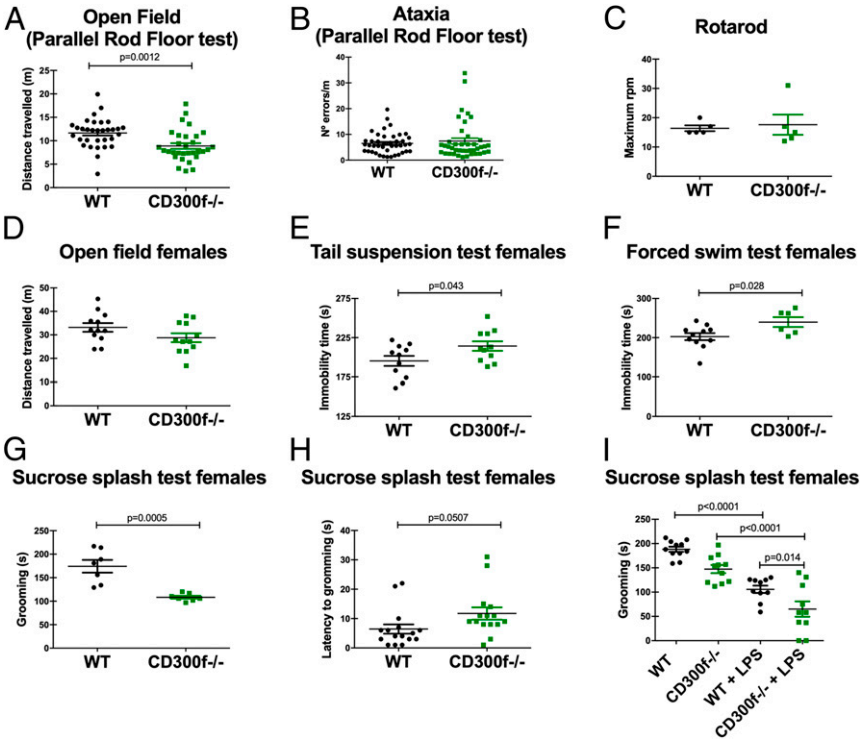

Fig. 2. CD300f$^{-/-}$ female mice display depressive-like and anhedonic phenotype. Adult (4 to 5 mo) male and female mice were evaluated for spontaneous locomotor activity in an open field arena (in the parallel rod floor test in *A*, or only females in a regular open field arena in *D*) and for motor impairment in the parallel rod floor test (for ataxia in *B*) or the rotarod (test with increased revolutions per minute is shown in *C*). The total immobility time in the TST in *E* and the FST in *F* was measured in females to evaluate depressive-like behavior. The total time in grooming behavior (*G*) and the latency to start grooming behavior (*H*) in the SST were recorded in females to evaluate motivational/self-care behavior and hedonic-like behavior, respectively. i.p. injection of LPS (2 mg/kg) induced 24 h after a potentiated anhedonic response in CD300f$^{-/-}$ female mice (*I*, two-way ANOVA followed by Bonferroni's post hoc test). Each dot represents a different animal and data are from at least two independent experiments. Data are represented as mean ± SEM.

behavioral phenotype consistent with depressive-like and anhedonic behaviors similar to that observed in adult CD300f$^{-/-}$ female mice (*SI Appendix*, Fig. S3). Taken together, these results show that the CD300f$^{-/-}$ female, but not male, mice display long-lasting behavioral alterations consistent with key behavioral symptoms associated with MDD in patients.

CD300f Deficiency and Neuroinflammation. The CD300f immune receptor is expressed in vitro in postnatal microglial cultures (38, 39). We isolated CD11b^{+}/CD45^{low} microglial cells from naïve spinal cord by fluorescence-activated cell sorting (FACS) (*SI Appendix*, Fig. S4 *A* and *B*), and qPCR for CD300f messenger RNA (mRNA) showed ~40-fold enrichment in the microglial fraction (*SI Appendix*, Fig. S4 *C* and *D*) when compared to total spinal cord extracts. These data are in accordance with mouse and human RNA sequencing (RNA-seq) experiments showing that CD300f mRNA is expressed only in microglia in the naïve CNS parenchyma and by CNS barrier macrophages (32, 40).

To understand the biological role of CD300f in the CNS, we first explored the hypothesis that it might participate in the regulation of microglial phenotype and restrain neuroinflammatory signals. We sorted CD11b^{+}/CD45^{low} microglial cells from the hippocampus of saline- or LPS-injected WT and CD300f$^{-/-}$ female mice and performed RNA-seq studies to compare their phenotype with the reported homeostatic microglial signature (8, 10, 32). Highly enriched microglial samples were obtained (*SI Appendix*, Fig. S5). The RNA-seq gene expression profiles of naïve WT and CD300f$^{-/-}$ microglia were slightly different, as observed by principal component analysis (Fig. 3*A*). In fact, only 34 genes were significantly differentially expressed (false discovery rate [FDR]-adjusted *P* value <0.1) between microglia from naïve WT and CD300f$^{-/-}$ mice (Fig. 3*B*). No significant alterations associated to KEGG (Kyoto Encyclopedia of Genes and Genomes) pathways were found for this dataset. When the homeostatic microglial gene signature was analyzed, we observed that CD300f deficiency did not alter expression of homeostatic genes (*SI Appendix*, Fig. S6*A*) and did not undergo a phenotypic shift toward a DAM phenotype (5, 6) (*SI Appendix*, Fig. S6*B*). Only one DAM and immature microglial marker gene, Spp1 (also termed osteopontin), showed a

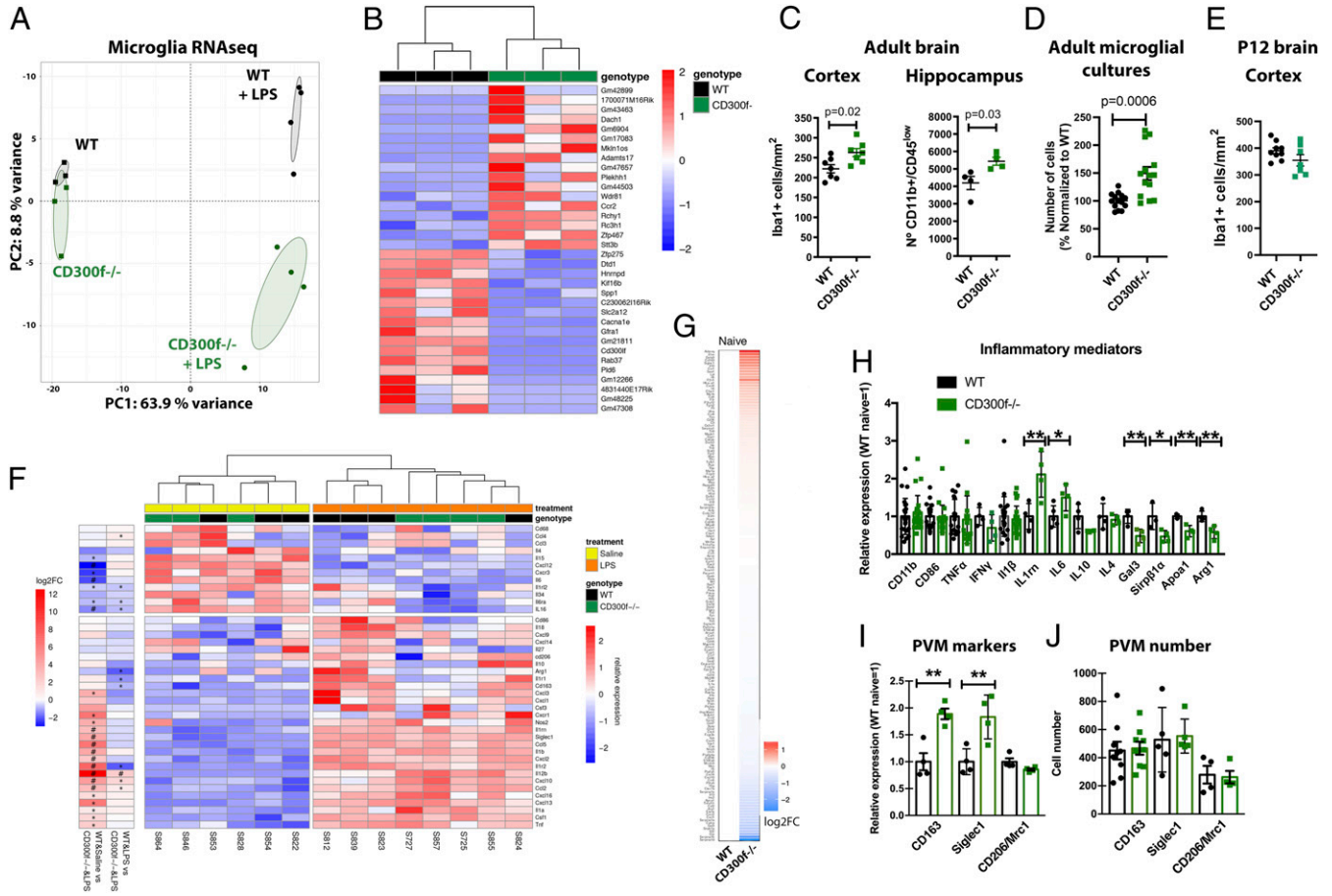

Fig. 3. Acutely isolated CD300$^{-/-}$ microglia show mild alterations in their transcriptome and increased numbers in the naïve hippocampus. The hippocampi of female WT and CD300f$^{-/-}$ mice injected with saline or LPS (2 mg/kg) were collected for the isolation of CD11b^{+}/CD45^{low} microglial cells by cell sorting. RNA-seq of mRNAs was undertaken, and the overall grouping by principal component analysis (PCA) is shown (*A*). PCA was based on the regularized expression levels of the 150 most variable genes, and the confidence ellipses were computed at the 0.9 level. The heat map of the 34 differentially expressed genes (P_{adj} < 0.1) among saline-injected WT and CD300f$^{-/-}$ is shown (*B*). Expression levels are shown scaled by row after regularized transformation of estimated values. CD300$^{-/-}$ adult mice cortex or hippocampus, but not P12 brain cortex (*E*), showed increased microglial cell density (IBA1+ cells by immunohistochemistry or CD11b^{+}/CD45^{low} cell by FACS, respectively (*C*). Adult CD300f$^{-/-}$ microglial cultures showed increased cell density (each dot represents a well of three independent cultures, *D*). Most inflammatory genes were not altered in CD300f$^{-/-}$ microglia in naïve conditions or after LPS injection (see selected genes in *F*), or in total brain and spinal cord extracts of naïve animals (*G* and *H*). Alterations in the mRNA of some perivascular macrophage markers were observed (*I*), while no changes in their cell number by FACS could be detected (*J*). Each dot represents a different animal in *C*, *E*, and *H*–*J*. Data are represented as mean ± SEM. Heat map in *F* as in *B* and additional log2 raw fold changes for specific combinations of genotypes and conditions are shown. In *F*, each * represents P_{adj} < 0.1; each # represents P_{adj} < 0.1 and abs(log2FC) ≥ 1 with P_{adj} < 0.1. In *H* and *I*, * and ** represent P < 0.05 and *P* < 0.01 respectively.

significant down-regulation. Interestingly, decreased serum Spp1 has been found in MDD patients (41).

While RNA-seq results showed no change in the main CD300f$^{-/-}$ microglial signature genes in naïve animals, we observed increased microglia numbers. Indeed, the direct cell counts of IBA1 immunoreactive cells in adult mice motor cortex showed an 18.3 ± 4.6% increase in CD300f$^{-/-}$ mice (Fig. 3*C*). These data were replicated in a different colony housed at the Universitat Autònoma de Barcelona, where FACS staining of CD11b^{+}/CD45^{low} hippocampal microglial cells showed a 29.8 ± 5.4% cell density increase in adult CD300f$^{-/-}$ mice (Fig. 3*C*). This increased CD300f$^{-/-}$ microglial cell division rate could be replicated in adult microglial purified cell cultures (Fig. 3*D*). In addition, in vivo, no differences could be detected by FACS staining for active Caspase 3 in WT and CD300f$^{-/-}$ mice (naïve WT: 1.50 ± 0.24 and CD300f$^{-/-}$: 1.48 ± 0.21; or i.p. LPS-treated WT: 1.19 ± 0.24 and CD300f$^{-/-}$: 1.03 ± 0.40, mean ± SEM). Thus, decreased levels of apoptosis in CD300f$^{-/-}$ microglia or increased apoptosis in WT microglia do not account for the in vivo increased microglial numbers. Interestingly, an increase in microglial density and a chronic microglial dysfunction has been associated with a dystrophic phenotype linked to psychiatric disorders, including MDD (1). The increase in microglial density in adult CD300f$^{-/-}$ brain occurs gradually, as no changes in microglial density was observed in postpartum day 12 (P12) mice when microglia has already stopped proliferating (32) (Fig. 3*E*). Taken together, these data suggest that CD300f$^{-/-}$ microglia maintain their homeostatic phenotype despite subtle changes in gene expression and cell number under naïve conditions. Moreover, the absence of CD300f immune receptor per se did not predispose microglial cells toward a proinflammatory phenotype.

While the absence of CD300f in microglial cells did not trigger a neuroinflammatory milieu, it could potentiate an externally induced neuroinflammatory process. To explore this hypothesis we used two well-described models of neuroinflammation that do not involve major blood–brain barrier disruption, tissue damage, or myeloid cell recruitment, i.p. LPS injection and peripheral nerve injury (42). When WT and CD300f$^{-/-}$ female mice were intraperitoneally injected with LPS, a differential expression of 1,304 microglial genes was observed (FDR-adjusted *P* value <0.1; Dataset S1). Interestingly, while LPS induced a well-known differential gene expression in WT microglia (see selected genes in Fig. 3*F*), most of the altered gene expression observed in the CD300$^{-/-}$ LPS-treated mice was not related to classical inflammatory mediators such as tumor necrosis factor α, IL-1β, nitric oxide synthase 2, or chemokines (see selected genes in Fig. 3*F*). In other words, among the 5,865 microglial differentially expressed genes after LPS treatment in WT animals (Wald test, FDR-adjusted *P* value <0.1), only 197 genes were altered by CD300f deficiency, and with a few exceptions (such as Arg1, IL-12β, or CCL12) were not classical neuroinflammatory mediators (Dataset S1 and *SI Appendix*, Fig. S7). Thus, the transcriptomic effect induced by LPS in WT animals was not potentiated or inhibited by the absence of CD300f, which instead showed a different profile. In accordance with the absence of widespread changes in inflammatory mediators after LPS injection, a peripheral sciatic nerve injury-induced neuroinflammation did not show enhanced spinal cord inflammation at different time points (from 2 to 28 d postlesion) in CD300f$^{-/-}$ mice compared to WT. This includes no changes in IBA1 microglial staining, Luminex cytokine measurements, or qPCR (*SI Appendix*, Fig. S8).

To further test the hypothesis that CD300f immune receptor could modulate neuroinflammation, we analyzed the expression levels of 179 inflammatory/phagocytic genes in the total spinal cord and brain extracts from naïve WT or CD300f$^{-/-}$ naïve animals of both sexes. No significant alterations in most of the analyzed genes were observed (Fig. 3 *G* and *H*). This finding is consistent with the modest alterations in global gene expression observed by RNA-seq in microglial cells. Interestingly, among the very few gene expression alterations observed in the naïve brains of the CD300f$^{-/-}$ animals were the increased mRNA for Il1rn and IL-6 (Fig. 3*H*), two well-documented MDD-associated cytokines (3, 4). Moreover, the CD300f$^{-/-}$ brains also showed alterations in the mRNA expression of Siglec1, Sirpβ1, and Apoa1, which in addition to Il1rn have been shown to be part of a gene coexpression module in MDD (43). Besides microglial cells, perivascular macrophages also express CD300f (5). The mRNA for two specific markers of these cells, CD163 and Siglec1 (5, 44), were increased in brain extracts of CD300f$^{-/-}$ animals (Fig. 3*I*), and interestingly CD163 has been described as a common marker of several psychiatric conditions including MDD (43). However, no changes were observed in the mRNA for CD206, another perivascular macrophage marker (Fig. 3*I*) (5, 44), or in the number of CD163+, Siglec1+, or CD206+ cells (Fig. 3*J*).

Altogether, these data suggest that CD300f$^{-/-}$ mice do not develop classical neuroinflammation but display several features of altered neuroimmune communications including increased microglial number, possible alterations in microglial and perivascular macrophage phenotype, and increased innate mediators such as Il1rn and IL-6, all previously associated to MDD.

Analysis of Microglial Phenotype Associated to the Depressive Phenotype. When WT and CD300f$^{-/-}$ female mice were intraperitoneally injected with LPS, CD300f deficiency worsened the depressive phenotype (Fig. 2*I*). Moreover, the transcriptomic effect induced by LPS in WT microglia was mainly maintained in CD300f$^{-/-}$ LPS-treated animals but they also showed additional transcriptomic changes (Fig. 3*A*), highlighting a different nonclassical proinflammatory mechanism for the induction or potentiation of the depressive-like phenotype. Interestingly, significant enrichment in KEGG pathways and Gene Ontology analysis of biological processes were found for this RNA-seq dataset mainly associated to autophagy and several metabolic pathways (Fig. 4*A* and *SI Appendix*, Fig. S9). Much recent evidence shows that receptor systems that mediate macrophage activation are linked to metabolic pathways, and that metabolic reprogramming is an integral part of the activation process (45). The adoption of the Warburg, or glycolytic metabolism, by macrophages is critical for their activation in response to LPS and other activators (46). Interestingly, we observed that key metabolic components were down-regulated in CD300f$^{-/-}$ microglia from LPS-treated animals when compared to WT LPS-treated mice (Fig. 4 *B* and *C*). This down-regulation impacted several pathways such as glycolysis (e.g., glucose transporters SLC2a1 and SLC2a3, also termed Glut1 and Glut 3 or hexokinase 1, Hk1; Fig. 4 *B* and *C*), gluconeogenesis (e.g., phosphoenolpyruvate carboxykinase 2, Pck2/Pepck2; Fig. 4 *B* and *C*), mitochondrial fatty acid β-oxidation (e.g., carnitine palmitoyltransferase 1a, Cpt1a; *SI Appendix*, Fig. S10), lipid synthesis (e.g., Acyl-CoA Synthetase Short Chain Family Member 2, Acss2), or Krebs cycle (e.g., Isocitrate dehydrogenase, Idh1, or mitochondrial pyruvate carrier 2, Mpc2; *SI Appendix*, Fig. S11). In many cases, the down-regulation of key enzymes in the CD300f$^{-/-}$ microglia of LPS-treated animals was even significant when compared with WT microglia, as observed for Hk1, Pck2, Idh1, or Acadm, among others (Fig. 4*B* and asterisks in Fig. 4*C*). In accordance, CD300f$^{-/-}$ microglia acutely isolated from LPS-treated mice showed reduced basal mitochondrial (Fig. 4*D*) and glycolytic activity (Fig. 4*E*). Moreover, the glycolytic shift normally observed in WT cells after the addition of mitochondrial stressors could not be induced in CD300f$^{-/-}$ microglia from LPS-treated mice (Fig. 4*E*). The total mitochondrial mass, however, did not differ between these two groups (Fig. 4 *F* and *G*), suggesting that mitochondrial dysfunction rather than lower mitochondrial content occurs in CD300f$^{-/-}$ microglia after peripheral LPS-induced activation. In accordance with our RNA-seq data and previous reports suggesting

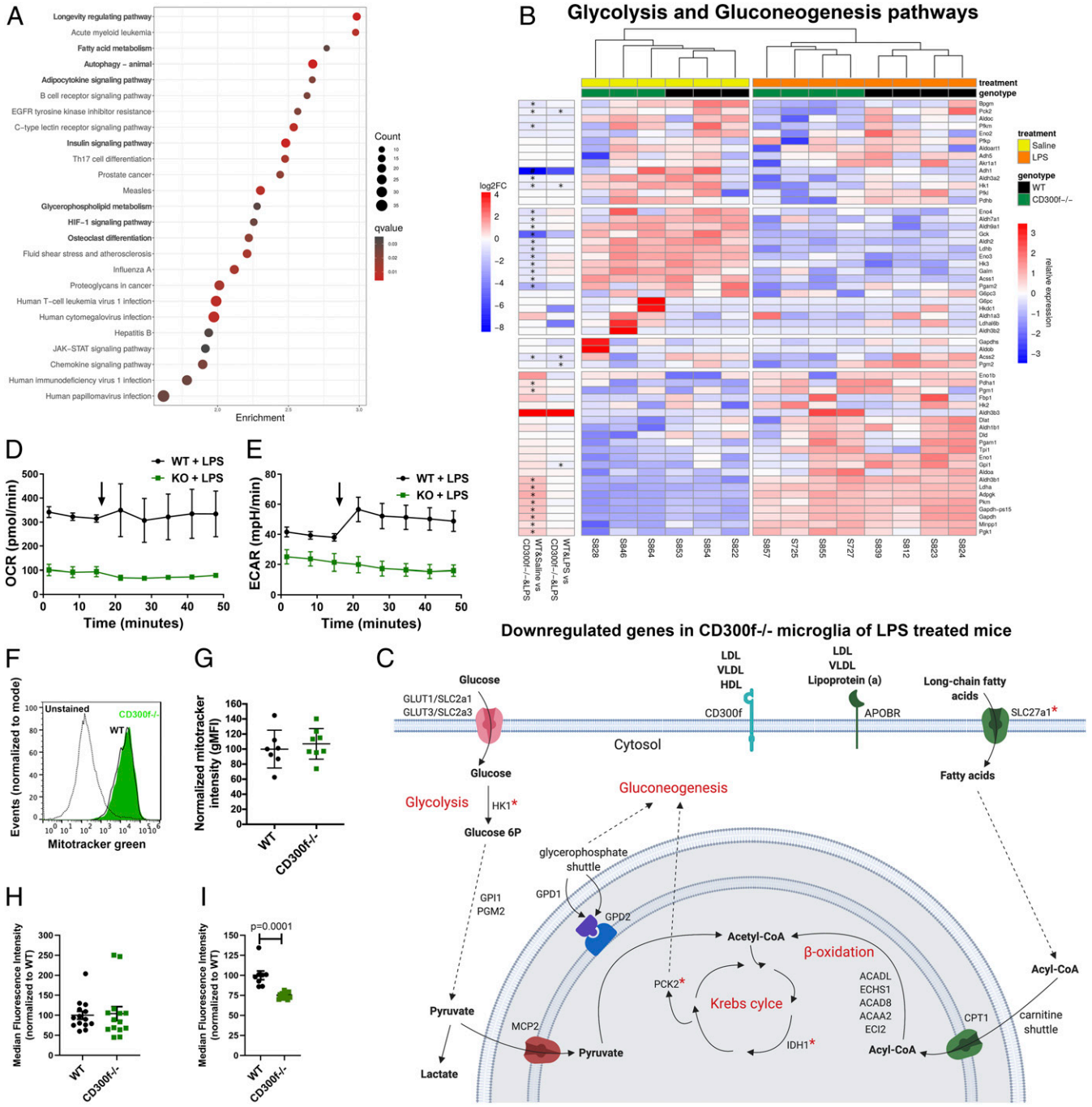

Fig. 4. Loss of CD300f$^{-/-}$ induces altered metabolic reprogramming of microglial cells. The hippocampi of female WT and CD300f$^{-/-}$ mice injected with saline or LPS (2 mg/kg) were collected for the isolation of CD11b^{+}/CD45^{low} microglial cells by cell sorting. RNA-seq of mRNAs was undertaken, and KEGG pathways enrichment analysis was performed on the list of differentially expressed genes for WT+LPS vs. CD300f$^{-/-}$+LPS (1,304 genes; FDR-adjusted P value <0.1, *A*). Expression profiles for the genes associated to the glycolysis and gluconeogenesis pathways were selected and the heat map show the expression levels scaled by row after regularized transformation of estimated values. Log2 raw fold changes for some specific combination of genotypes and conditions are shown. Each * represents $P_{adj} < 0.1$; each # represents $P_{adj} < 0.1$ and abs(log2FC) ≥ 1 with $P_{adj} < 0.1$ (*B*). A schematic representation of key metabolic pathway genes down-regulated in LPS-injected CD3000$^{-/-}$ versus LPS-injected WT mice (*C*, red asterisks represent genes also down-regulated when compared to saline-injected WT mice). Seahorse experiments using acutely isolated CD11b^{+} hippocampal microglial cells by magnetic beads were performed, and the oxygen consumption rate (*D*) and extracellular acidification rate (*E*) were measured. FACS analysis of CD11b^{+}/CD45^{low} microglial cells with MitoTracker Green for estimating the mitochondrial mass was undertaken (*F* and *G*). Phagocytosis of fluorobeads (*H*) and endocytosis of pHrodo-LDL (*I*) was analyzed in WT and CD300f$^{-/-}$ adult microglial purified cultures. VLDL, very-low-density lipoprotein.

that CD300f may act as a lipoprotein receptor, CD300f$^{-/-}$ microglia showed a decreased receptor-mediated LDL endocytosis, while no alteration on nonreceptor-mediated phagocytosis was detected (Fig. 4 *H* and *I*). Moreover, key microglial transcription factors such as Mafb, Egr1, Maf1, and Cebpg were down-regulated and differential expression of 23 genes of the autophagy pathway were observed in the CD300f$^{-/-}$ microglia from LPS-injected animals (*SI Appendix*, Fig. S12). Collectively, these data suggest that the

metabolic reprogramming needed for microglial activation is compromised in CD300f$^{-/-}$ mice, and that this also alters autophagy processes, in a similar fashion as TREM2$^{-/-}$ microglia in an Alzheimer's disease model (11).

CD300f Modulates Synaptogenesis and Synaptic Strength In Vitro by a Glial-Mediated Mechanism. Microglia have been associated with synaptic pruning and modulation of neurotransmission (47). To evaluate how microglial CD300f might be involved in neurotransmission alterations, we analyzed the effect of blocking CD300f on the modulation of synaptogenesis and excitatory synaptic strength in mixed neuron–glia hippocampal cultures. The cultures were stained for the presynaptic and postsynaptic markers vGlut1/Homer, respectively (Fig. 5 *A* and *B*). Moreover, we measured the intensity of synaptic vGlut1 immunoreactivity, which was shown to accurately estimate the probability of neurotransmitter release (48) and thus of synaptic strength. Incubation of cultures with tetrodotoxin (TTX) induced the well-described synaptogenesis/synaptic plasticity (49) evidenced by an increased number of total vGlu1/Homer-positive synapses (Fig. 5*C*), as well as an increased intensity of individual presynaptic vGlut1 immunoreactivity (Fig. 5*D*). Similarly, the addition of the soluble competitive inhibitor CD300f-Fc fusion protein to these cultures at concentrations comparable (0.01 μg/mL) to the soluble CD300f form produced by microglia in culture (39) also induced an increase in the total number of synapses and in the probability of neurotransmitter release (Fig. 5 *C* and *D*). Under these conditions, no neuronal cell death was detected (*SI Appendix*, Fig. S13*A*). To determine if this effect was mediated by glial cells, hippocampal neuron-enriched cultures were incubated directly with rCD300f-Fc, or alternatively with conditioned medium from mixed glial cultures treated with rCD300f-Fc. Interestingly, no changes in the number of synapses (*SI Appendix*, Fig. S13*B*) or in the probability of release (*SI Appendix*, Fig. S13*C*) could be observed in hippocampal neuron cultures treated directly with rCD300f-Fc or with the different mixed glial conditioned media. Taken together, these results suggest that CD300f may be involved in the turnover of synapses and regulation neurotransmission by a glial and contact-dependent mechanism.

Hippocampal Noradrenaline Level-Dependent Depressive Phenotype of CD300f-Deficient Animals. MDD has been classically associated with decreased levels of serotonin, dopamine, and noradrenaline in brain regions involved in mood regulation such as the hippocampus (50). Alteration of microglial-mediated synaptic plasticity could alter neurotransmitter levels. To evaluate if the behavioral changes observed in female CD300f$^{-/-}$ mice are associated with changes in monoaminergic neurotransmission, the levels of serotonin, dopamine, and noradrenaline were analyzed in the hippocampus. Interestingly, hippocampal noradrenaline was significantly decreased, whereas no other significant changes were observed in the levels of serotonin or dopamine (Fig. 5 *E*–*G*). This decrease has been associated with some forms of MDD (50). The reduction in noradrenaline was due to neurotransmitter content, as no alteration was observed in noradrenergic projections in the hippocampus (*SI Appendix*, Fig. S13 *D*–*F*). Importantly, the administration of bupropion, a selective noradrenaline and dopamine uptake inhibitor used as antidepressant in the clinic, reversed the anhedonic behavior in CD300f$^{-/-}$ female animals but did not affect the WT (Fig. 5*H*). Taken together, these data suggest that CD300f may participate in microglial-mediated neuroplasticity and, when altered, induce a noradrenaline-dependent depressive-like phenotype.

Discussion

The main finding of this work indicates that the functional status of the CD300f immune receptor influences the development of MDD in both female mice and female humans. In mice, this persistent effect occurs in the absence of overt neuroinflammation and is associated to increased microglial cell number, alterations in several MDD-related cytokines (IL-6, IL1rn, and Spp1) and cell

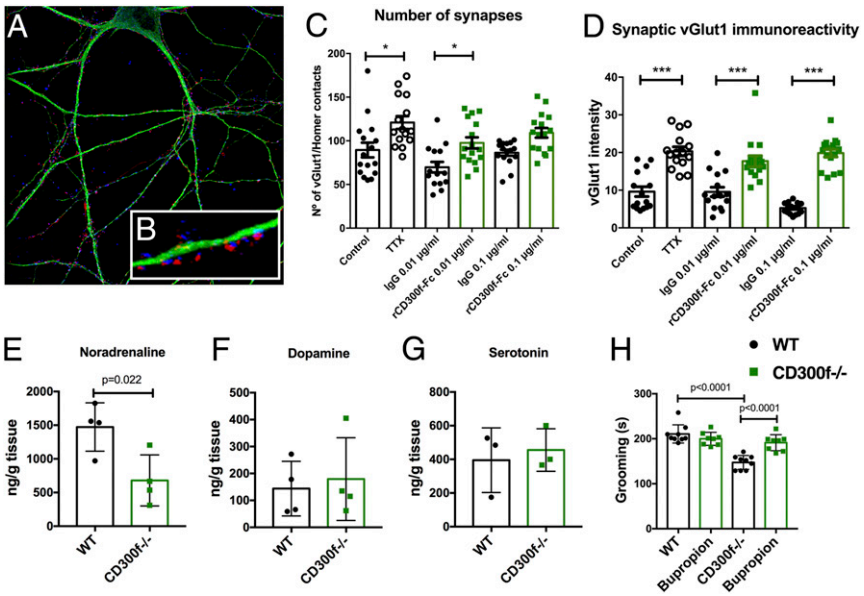

Fig. 5. Loss of CD300f$^{-/-}$ alters synaptic strength and reduces noradrenaline levels in the hippocampus. Mixed hippocampal–glial cocultures (36.2 ± 5.1% neurons, 11.4 ± 0.7% microglia, 37.7 ± 4.4% astrocytes and 14.8 ± 3.2% oligodendrocytes) were treated with recombinant CD300f-Fc fusion protein, immunoglobulin G (IgG) isotype control, or TTX. The number of synaptic contacts (partial colocalization of vGlut1 and Homer, *A*–*C*) and the synaptic strength (vGlut1 staining intensity in each of these synaptic contacts, *D*) were quantified. Data are from two independent experiments run in duplicate, and $n = 8$ neurons per well were analyzed in *C* and *D*. Data are represented as mean ± SEM. Female mice were perfused with saline and the hippocampus extracted for the analysis of different neurotransmitter levels by HPLC (*E*–*G*). Administration of bupropion (10 mg/kg i.p.) reversed the anhedonic behavior in the SST (*H*, two-way ANOVA followed by Bonferroni's post hoc test). Each dot represents a different animal and data in *H* are from two independent experiments.

markers (CD163), and modulation of synaptic strength and is dependent on hippocampal noradrenergic neurotransmission. Moreover, the CD300f immune receptor emerges as a central regulator of microglial immunometabolic reprogramming and, in conjunction with perivascular macrophage phenotype alterations, may contribute to the depressive-like phenotype.

CD300f Immune Receptor Is Involved in MDD. Association of inflammation and depression has been well documented both in animal models and clinical studies (36, 51). MDD frequently accompanies patients suffering from sustained systemic inflammation (52, 53). It was also recently proposed that TREM2, which shares most of its ligands with CD300f (17–19), may act as a CNS damage-associated molecular pattern (DAMP) receptor or neurodegeneration-associated molecular pattern receptor (54). Several DAMPs and their receptors have been associated to MDD (55). Thus, CD300f could also function as a DAMP receptor modulating microglial and perivascular macrophage phenotype. We hypothesized that in the absence of a restraining signal (CD300f), microglial and perivascular macrophages would induce low-grade neuroinflammation that could lead to a depressive-like behavior. Interestingly, the absence of CD300f led to depressive-like and anhedonic behaviors, but this was not associated with overt neuroinflammation. In fact, qPCR mRNA profiling for proinflammatory gene expression in the whole brain or RNA-seq of sorted microglial cells showed no significant changes in most of the genes analyzed. In addition, microglia demonstrated no evident morphological alterations, and the signature mRNA levels for infiltrating cells such as CD4 (subset of T lymphocytes), Mpo (neutrophils), and Il17a (Th17 cells) remained stable, suggesting no infiltration of these cells. Interestingly, while no changes in the number of perivascular macrophages were observed in the CNS of CD300f$^{-/-}$ animals, two of their most specific markers, CD163 and Siglec1 (5, 44), showed increased mRNA expression, arguing in favor of a phenotypic change in this cell type. Interestingly, transcriptomic profiling showed that increased expression of CD163 is found among the top 40 common genes altered in several major psychiatric conditions, including MDD, bipolar disorder (BP), autism spectrum disorder (ASD), schizophrenia (SCZ), or alcohol abuse disorder (AAD), and both CD163 and Siglec1 are included in a MDD coexpression network (43). Moreover, individuals that committed suicide displayed increased density of perivascular macrophages (56, 57). This suggests that perivascular macrophages may have a role in MDD and that functional alteration of these cells in CD300f$^{-/-}$ mice might contribute to the depressive phenotype. This warrants further studies to explore the hypothesis that alterations in CNS tissue resident macrophages contribute to MDD and other psychiatric conditions.

The three different CD300f$^{-/-}$ mice models generated to date did not show any alterations in the immune system or inflammatory markers in the systemic circulation (20, 30, 35), even at 15 mo of age (35). In agreement with the lack of inflammation observed in the CD300f$^{-/-}$ mice, patients carrying the T allele of the rs2034310 SNP and showing protection against MDD did not show alterations in IL-1β protein levels in serum when compared to the other genotypes, suggesting that the mechanism by which CD300f acts during MDD may not be related to classical inflammatory processes. Interestingly, several reports have shown important noninflammatory intricate neuroimmune communications during development, homeostasis, and neurological diseases (58). In fact, among the very few genes found to be upregulated in the brains of naïve CD300f$^{-/-}$ mice were Il1ra (IL1rn), the soluble inhibitor of IL-1α and IL-1β signaling, and also IL-6, the two most common cytokines previously shown to be selectively increased in serum of MDD patients (3, 4). In this sense, CD300f may contribute to neuroimmune communication in several ways aside from the regulation of the classical neuroinflammatory pathways.

Previously published epidemiological data showed that women are more susceptible to MDD than men (59), and the data we obtained in the population-based study reported here are in accordance. Strikingly, absence of CD300f only induced a depressive-like phenotype in female mice and not in males. Moreover, the protection against MDD conferred by the T allele of CD300f rs2034310 SNP in humans showed significant differences in women but not men. This difference may be due to a limited power of analysis in the male cohort or instead point to a true gender difference. This intriguing effect needs to be studied further in a larger patient cohort. The observation that the T allele of CD300f rs2034310 SNP confers protection against MDD in humans has several important implications. The mechanism by which this protection occurs implies a dominant effect, as only one T allele is needed in heterozygosis. The C/T exchange produces a nonsynonymous substitution of arginine to glutamine in the cytoplasmic tail of the receptor and we show here that this alters the physiological signaling of CD300f mediated by PKCδ phosphorylation. Additional studies are needed to further understand the functional implications of this substitution.

CD300f and the Modulation of Neurotransmission. The most widely accepted hypothesis for the etiology of MDD at the neurochemical level is dysfunctional monoaminergic neurotransmission, mainly of serotonin, in several brain regions of MDD patients. However, clinical and experimental observations show that this constitutes a reductionist view, and that a more complex view includes alterations in other neurotransmitters (e.g., noradrenaline and dopamine), in neurotrophic factors (e.g., brain-derived neurotrophic factor), neurogenesis, and the hypothalamic–pituitary–adrenal axis (60). Our results show that the CD300f$^{-/-}$ female mice have reduced hippocampal noradrenaline content, but not of dopamine or serotonin. When the neurons of the locus coeruleus, the main source of noradrenergic neurons in the brain, are activated by an arousal or a novelty, noradrenaline is released in the hippocampus, and in accordance with the data observed here its activity is down-regulated in MDD (61). Interestingly, the administration of the antidepressant bupropion, which selectively inhibits the uptake of noradrenaline and dopamine, raising its extracellular levels at the synapses, reversed the anhedonic behavior of the CD300f$^{-/-}$ female mice. In humans, chronic treatment with antidepressants was shown to reduce binding of the TSPO PET ligand [18F]FEPPA in the brains of MDD patients, likely reflecting decreased microglial and perivascular macrophage reactivity or cell number (2) and associating microglial phenotype with antidepressant action.

Deficiency in microglial receptors such as CX3CR1 (15) and TREM2 (62) cause alterations in synaptic transmission and social behavior. Interestingly, the inhibition of the endogenous CD300f in mixed hippocampal cultures modulated synaptic strength and synaptogenesis. One of the main functions of CD300f as an activating receptor is to enhance macrophage efferocytosis by phosphatidylserine ligation in apoptotic cells, contributing to tissue clearance and resolution of inflammatory processes (26). This mechanism of phagocytosis could potentially also be used for the engulfment of dendritic spines or axonal terminals (63), which would result in the observed increased number of synapses following inhibition of CD300f. In addition, microglial CD300f could also bind the phospholipids of the ApoE lipoprotein (64) and prune synapses by this mechanism. In favor of this hypothesis, we show that the mechanism of the modulation of synaptic strength and number is both contact- and glial-dependent. Alternatively, CD300f may modulate microglial immunometabolic reprogramming and indirectly modulate phagocytosis and synaptic pruning. In line with this hypothesis, it has been shown that alterations in cerebral metabolism in MDD patients is more frequent in women

than in men (65), and creatine, a metabolic stimulator, has antidepressive effects in female (but not male) rats (66) and in women (67). Interestingly, a recent report shows that the knockout of TREM2 or PGRN, two mainly microglial genes, can modulate whole-brain metabolism (68), suggesting that the CD300f knockout may lead to widespread brain metabolic alterations.

CD300f and the Regulation of the Microglial Phenotype. A recent report includes CD300f in the list of genes putatively constituting the microglial reactome, a group of microglial genes coregulated in response to several classical neuroinflammatory triggers such as LPS, kainic acid-induced status epilepticus, and the presymptomatic superoxide dismutase amyotrophic lateral sclerosis model (69). As described before (32), after an i.p. LPS injection in WT mice CD300f was up-regulated and among the most significant differentially expressed genes (37th of 5,866). We observed that the CD300f deficiency induces an increase in microglial number in the absence of major changes in microglial signature genes or dysregulation of DAM genes. This suggests that the mild changes in microglial phenotype observed here under naïve conditions, and associated with a psychiatric condition, may differ from the more stereotyped phenotype associated to neurodegenerative conditions. Although several studies analyzing the transcriptome of psychiatric conditions have been published (43), a microglial-specific transcriptome for MDD or other psychiatric conditions is still missing. Interestingly, the fact that only mild changes occur in the set of genes analyzed between WT and CD300f$^{-/-}$ animals is in line with the subtle changes in gene expression patterns observed in MDD patients when compared to ASD, SCZ, BP, or AAD (43). Accordingly, although very mild microglial transcriptomic changes were observed in TREM2$^{-/-}$ (30 to 40 genes) (18) or Hoxb8$^{-/-}$ animals (21 genes) (70), they display alterations in microglial synapse elimination and social interaction or in obsessive–compulsive behavior, respectively. A relevant question is when the cellular changes occur. The mild microglial transcriptomic changes observed in CD300f$^{-/-}$, TREM2$^{-/-}$, or Hoxb8$^{-/-}$ mice could be masking more dramatic changes occurring during development, as reported previously in other models of psychiatric disorder involving microglia (71).

In conclusion, we demonstrate a clear association between the CD300f immune receptor with MDD in women as well as depressive-like and anhedonic behaviors in female mice only. Our findings reinforce the notion that a significant amount of the genetic load, which influences the development of depression, may exert its function through microglia. Importantly, CD300f emerges as a central player in the metabolic reprogramming needed for microglial activation. Despite the high incidence in MDD, no effective treatments are available in many cases, and these discoveries could lead to the development of new pipelines for drugs targeting microglial cells, perivascular macrophages, and in particular CD300f immune receptor.

Methods

Animals. Adult (4 to 5 mo old) female or male C57BL/6 (Charles River) WT mice and CD300f$^{-/-}$ [Genentech (30)] mice were obtained from the SPF animal facility of Institut Pasteur de Montevideo-Uruguay. Animals were maintained under controlled environment (20 ± 1 °C, 12-h light/dark cycle, free access to food and water).

Cell Sorting of Microglia. Mice were deeply anesthetized with sodium pentobarbitone (100 mg/kg, i.p.) and perfused with ice-cold PBS to eliminate blood. Spinal cord or hippocampus was harvested and cut in small pieces and enzymatic digestion was performed for 30 min at 37 °C. The digested tissue was passed through a cell strainer (40 μm, Falcon; BD Bioscience Discovery Labware), and the cell suspension was centrifuged at 500 × *g* for 10 min at 4 °C. The supernatant was discarded and cells resuspended in 2 mM EDTA and 0.5% fetal bovine serum (FBS) in phosphate-buffered saline (PBS). Cells were incubated with anti-CD11b MicroBeads (1:10, 130-049-601; Miltenyi Biotec) for 15 min at 4 °C and then applied to a magnetic LS column (Miltenyi Biotec). Cells retained on the column were flushed and resuspended in appropriate buffer and incubated with CD11b-PECy7 (1:200; eBioscience) and CD45-PerCP (1:200; eBioscience) for 1 h at 4 °C. The final pellet was resuspended in PBS and 2% FBS and subjected to flow cytometry. The sorting was performed using a FACSARIA III (BD Bioscience) cell sorter. We obtained about 30,000 purified cells from hippocampus samples and about 230,000 purified cells from whole brain. Microglial cells were assessed on a flow cytometer (FACS Calibur; BD Biosciences) and only populations presenting >90% purity were used for gene expression analysis. Sorted cells were directly collected in RLT buffer (QIAGEN) and RNA extraction was performed immediately after cell sorting to avoid RNA degradation. For LPS-induced neuroinflammation, LPS (2 mg/kg) was injected intraperitoneally 16 h before the RNA harvesting.

Metabolic Rate and Mitochondrial Mass Measurements. Four-month-old CD300f$^{-/-}$ and WT female mice were intraperitoneally injected with a single injection of LPS at 2 mg/kg. Twenty-four hours after injection, mice were deeply anesthetized with sodium pentobarbital (Dolethal) and transcardially perfused with 60 mL of 0.9% NaCl in distilled water. Whole brains were obtained and maintained in DMEM (Thermo Fisher Scientific) at 4 °C. Cell suspensions from brains were obtained as described above for FACS. Cells were then magnetically labeled with CD11b microbeads (MACS Miltenyi) and loaded onto LS MACS columns (Miltenyi Biotec) following the recommended protocol. CD11b+ cells were plated in an XFp cell culture miniplate (Agilent) following the protocol for cells suspensions. Seahorse XF Base Medium (Agilent) supplemented with 1 mM pyruvate (Sigma-Aldrich), 2 mM glutamine (Sigma-Aldrich), and 25 mM glucose (Sigma-Aldrich) was used. A mixture of oligomycin (1 μM) and FCCP (1.5 μM) was loaded into the proper cartridge (Agilent). Measurements of extracellular acidification rate and oxygen consumption rate from live cells were performed using the Seahorse XFp Cell Energy Phenotype protocol in a XFp Analyzer (Agilent). Three measures were taken under basal conditions and five measures after addition of oligomycin and FCCP. Final values were normalized by the amount of DNA loaded in every well. Three mice per group were used.

RNA-Seq and Data Analysis. Library preparation and RNA-seq were performed by the Centro Nacional de Análisis Genómico Centre for Genomic Regulation following the SMARTseq2 protocol (72) with some modifications. Briefly, RNA was quantified using the Qubit RNA HS Assay Kit (Thermo Fisher Scientific) and the input material used for the initial complementary DNA (cDNA) synthesis varied in function of the available sample concentration (0.2 to 10 ng). Reverse transcription was performed using SuperScrpit II (Invitrogen) in the presence of oligo-dT30VN (1 μM; 5′-AAGCAGTGGTATCAACGCAGAGTACT30VN-3′), template-switching oligonucleotides (1 μM), and betaine (1 M). The cDNA was amplified using the KAPA Hifi Hotstart ReadyMix (Kappa Biosystems), 100 nM ISPCR primer (5′-AAGCAGTGGTATCAACGCAGAGT-3′), and 15 cycles of amplification. Following purification with Agencourt Ampure XP beads (1:1 ratio; Beckmann Coulter), product size distribution and quantity were assessed on a Bioanalyzer High Sensitivity DNA Kit (Agilent). The amplified cDNA (200 ng) was fragmented for 10 min at 55 °C using Nextera XT (Illumina) and amplified for 12 cycles with indexed Nextera PCR primers. The Nextera library was purified twice with Agencourt Ampure XP beads (0.8:1 ratio) and quantified again on a Bioanalyzer using a High Sensitivity DNA Kit.

The libraries were sequenced on HiSeq2500 (Illumina, Inc.) in paired-end mode with a read length of 2 × 76 bp using TruSeq SBS Kit v4 and Nextera XT Index Kit of 8 bp + 8 bp. We generated on average 45 million paired-end reads for each sample in a fraction of a sequencing v4 flow cell lane, following the manufacturer's protocol. Image analysis, base calling, and quality scoring of the run were processed using the manufacturer's software Real Time Analysis (RTA 1.18.66.3) and followed by generation of FASTQ sequence files by CASAVA. See *SI Appendix* for data analysis procedures. Gene expression data for the different performed comparison are shown in Dataset S1. Raw data from the RNA-seq experiment have been deposited in the NCBI Sequence Read Archive under accession no. PRJNA496060.

Behavioral Analysis. Adult female and male WT and CD300f$^{-/-}$ mice (4 to 5 mo old, 35 to 40 g) were used for behavior analysis. All behavior experiments were performed during the illuminated part of the cycle under conditions of dimly lit by a red lamp and low noise. Behavior was monitored and videotaped to be scored later by a blind trained observer. For LPS induced depression experiments, LPS (2 mg/kg) was injected intraperitoneally 24 h before the behavioral tests.

OFT. The OFT was performed in order to assess the locomotor activity of mice. The apparatus consisted of an acrylic white box measuring 40 cm × 60 cm × 50 cm high. The animals were exposed during 6 min to the arena and the total distance traveled was recorded and evaluated using the AnyMaze software. The arena was cleaned with 10% alcohol between animals in order to exclude possible clues.

TST. Mice were submitted to the TST, which is a moderately stressful inescapable situation and despair model, where they are suspended by the tail and the depressive-like behavior can be evaluated. The lack of attempts to escape the aversive situation is considered immobility. In order to perform the TST, mice were suspended by the tail above the floor by adhesive tape ∼1 cm by the tip of the tail and the immobility time (in seconds) was recorded and evaluated during 6 min.

FST. The FST is a model of behavioral despair generally used in the evaluation of antidepressant or depressant effects of compounds or manipulations. In this test each mouse was individually forced to swim in an open cylindrical container (10 cm diameter × 25 cm high) containing ∼19 cm deep of water at 25 ± 1 °C and the immobility time was recorded during 6 min. In this test, mobility is defined when mice executed vigorous movements in order to get out of the acute stressful situation. Small movements executed by the animals just to keep balance or to keep the head above the water were not considered mobility.

SST. In this test, a 10% sucrose solution was spread on the dorsal coat of the mice. This viscose solution dirties the animal and they initiate grooming behavior. After applying the sucrose solution, the animals were individually placed in glass recipients and taped during 5 min. The latency to start the first grooming and the total amount of grooming behavior were the parameters associated with motivational behavior and anhedonic and self-care behavior, respectively. The recipients were cleaned with 10% ethanol between animals to exclude possible olfactive clues. The treatment with bupropion (10 mg/kg intraperitoneal, generously donated by Gramón Bagó Laboratories) or vehicle (PBS) was performed 30 min prior to the sucrose splash test.

Clinical study. This included a cross-sectional population-based study comprising 1,110 subjects aged 18 to 35 y and enrolled in a study carried out in the city of Pelotas, Southern Brazil, between June 2011 and May 2013. Sample selection was performed by multistage clusters, considering a population of 97,000 individuals in the 495 census-based sectors in the city. To ensure the necessary sample inclusion, 82 census-based sectors were systematically drawn. After identification, participants received morning visits by trained researchers in order to collect sociodemographic and clinical information. Several variables such as ethnicity and the use of psychiatry medication were self-reported. Subjects were diagnosed with the MDD (current or past episode) using the structured diagnosis interview, the Mini International Neuropsychiatric Interview according to DSM-IV criteria (M.I.N.I. 5.0., Brazilian version/DSM-IV; Medical Outcome Systems, Inc.).

Study approval. Studies including animals were performed according to the guidelines of the Institut Pasteur de Montevideo Animal Care Committee (protocols 004-16 and 014-16) and following the guidelines of the European Commission on Animal Care and Uruguayan national law and ethical guidelines on animal care. The study including human patients was approved by the Ethics Committee of the Catholic University of Pelotas (2010/15) and all patients provided written informed consent to participate.

Statistics. Allelic frequencies were determined by gene counting, and departures from the Hardy–Weinberg equilibrium were verified using χ^2 tests. Comparisons of allelic and genotype frequencies between MDD patients and control subjects were evaluated using χ^2 tests. Sociodemographic characteristics according to diagnosis and genotype were analyzing by χ^2 tests. Continuous variables were evaluated using Student's *t* test, one-way ANOVA, or two-way ANOVA for repeated measures followed by Bonferroni's post hoc test, as appropriate. The magnitude of the association of different genotypes with MDD was estimated using OR tests with 95% CI, adjusting for age and ethnicity in logistic regression analysis. Bonferroni's correction was used to account for multiple comparisons. Statistical analyses were performed with the Statistical Program for Social Sciences (SPSS) statistical software version 20.0 and data were presented as mean ± SEM or percentage, considering $P < 0.05$ as statistically significant.

Data Availability. The raw data from RNA-seq are available in the NCBI Sequence Read Archive under accession no. SRA PRJNA496060 and in Dataset S1.

ACKNOWLEDGMENTS. This work was supported by grants from Fundació Marató TV3 (110533-110532), Catalunya, Spain; Comisión Sectorial de Investigación Científica, Uruguay; Programa de Desarrollo de las Ciencias Básicas, Uruguay; Fondo de Convergencia Estructural del MERCOSUR (COF 03/1111); Banco de Seguros del Estado, Uruguay; Spanish Ministry of Economy and Competitiveness (SAF2010-17851and SAF2013-48431-R); Red Española de Terapia Celular; Conselho Nacional de Desenvolvimento Científico e Tecnológico (CNPq); Coordenação de Aperfeiçoamento de Pessoal de Ensino Superior (CAPES); and Programa de Apoio a Núcleos de Excelência-Fundação de Amparo à Pesquisa do Estado do Rio Grande do Sul (08/2009 - Pronex 10/0055-0). Gramón Bagó Laboratories (Uruguay) donated the bupropion. R.A.S., D.R.L., K.J., L.M.S., and M.P.K. are CNPq Research Fellows. F.N.K. received a fellowship from CAPES and support from International Brain Research Organization and International Society for Neurochemistry. We thank all members of the transgenic animal unit (UATE) and of the Cell Biology Unit (especially Paula Céspedes) of the Institut Pasteur de Montevideo for assistance and Iris Castillo, Bruno Borrelli, and Camila Julian.

1. R. Yirmiya, N. Rimmerman, R. Reshef, Depression as a microglial disease. *Trends Neurosci.* **38**, 637–658 (2015).
2. E. Setiawan *et al.*, Association of translocator protein total distribution volume with duration of untreated major depressive disorder: A cross-sectional study. *Lancet Psychiatry* **5**, 339–347 (2018).
3. M. Maes *et al.*, Increased serum IL-6 and IL-1 receptor antagonist concentrations in major depression and treatment resistant depression. *Cytokine* **9**, 853–858 (1997).
4. C. A. Köhler *et al.*, Peripheral cytokine and chemokine alterations in depression: A meta-analysis of 82 studies. *Acta Psychiatr. Scand.* **135**, 373–387 (2017).
5. H. Keren-Shaul *et al.*, A unique microglia type associated with restricting development of Alzheimer's disease. *Cell* **169**, 1276–1290.e17 (2017).
6. S. Krasemann *et al.*, The TREM2-APOE pathway drives the transcriptional phenotype of dysfunctional microglia in neurodegenerative diseases. *Immunity* **47**, 566–581.e9 (2017).
7. K. Grabert *et al.*, Microglial brain region-dependent diversity and selective regional sensitivities to aging. *Nat. Neurosci.* **19**, 504–516 (2016).
8. S. E. Hickman *et al.*, The microglial sensome revealed by direct RNA sequencing. *Nat. Neurosci.* **16**, 1896–1905 (2013).
9. A. Crotti, R. M. Ransohoff, Microglial physiology and pathophysiology: Insights from genome-wide transcriptional profiling. *Immunity* **44**, 505–515 (2016).
10. O. Butovsky *et al.*, Identification of a unique TGF-β-dependent molecular and functional signature in microglia. *Nat. Neurosci.* **17**, 131–143 (2014).
11. T. K. Ulland *et al.*, TREM2 maintains microglial metabolic fitness in Alzheimer's disease. *Cell* **170**, 649–663.e13 (2017).
12. R. M. Ransohoff, A. E. Cardona, The myeloid cells of the central nervous system parenchyma. *Nature* **468**, 253–262 (2010).
13. A. Deczkowska, I. Amit, M. Schwartz, Microglial immune checkpoint mechanisms. *Nat. Neurosci.* **21**, 779–786 (2018).
14. F. Filipello *et al.*, The microglial innate immune receptor TREM2 is required for synapse elimination and normal brain connectivity. *Immunity* **48**, 979–991.e8 (2018).
15. Y. Zhan *et al.*, Deficient neuron-microglia signaling results in impaired functional brain connectivity and social behavior. *Nat. Neurosci.* **17**, 400–406 (2014).
16. A. W. Corona *et al.*, Fractalkine receptor (CX3CR1) deficiency sensitizes mice to the behavioral changes induced by lipopolysaccharide. *J. Neuroinflammation* **7**, 93 (2010).
17. S. C. Choi *et al.*, Cutting edge: Mouse CD300f (CMRF-35-like molecule-1) recognizes outer membrane-exposed phosphatidylserine and can promote phagocytosis. *J. Immunol.* **187**, 3483–3487 (2011).
18. Y. Wang *et al.*, TREM2 lipid sensing sustains the microglial response in an Alzheimer's disease model. *Cell* **160**, 1061–1071 (2015).
19. K. Izawa *et al.*, Sphingomyelin and ceramide are physiological ligands for human LMIR3/CD300f, inhibiting FcεRI-mediated mast cell activation. *J. Allergy Clin. Immunol.* **133**, 270–3.e1-7 (2014).
20. K. Izawa *et al.*, The receptor LMIR3 negatively regulates mast cell activation and allergic responses by binding to extracellular ceramide. *Immunity* **37**, 827–839 (2012).
21. A. Martínez-Barriocanal, E. Comas-Casellas, S. Schwartz, Jr, M. Martín, J. Sayós, CD300 heterocomplexes, a new and family-restricted mechanism for myeloid cell signaling regulation. *J. Biol. Chem.* **285**, 41781–41794 (2010).
22. D. Alvarez-Errico *et al.*, IREM-1 is a novel inhibitory receptor expressed by myeloid cells. *Eur. J. Immunol.* **34**, 3690–3701 (2004).
23. D. Alvarez-Errico, J. Sayós, M. López-Botet, The IREM-1 (CD300f) inhibitory receptor associates with the p85alpha subunit of phosphoinositide 3-kinase. *J. Immunol.* **178**, 808–816 (2007).
24. K. Izawa *et al.*, An activating and inhibitory signal from an inhibitory receptor LMIR3/CLM-1: LMIR3 augments lipopolysaccharide response through association with FcRgamma in mast cells. *J. Immunol.* **183**, 925–936 (2009).
25. I. Moshkovits *et al.*, CD300f associates with IL-4 receptor and amplifies IL-4-induced immune cell responses. *Proc. Natl. Acad. Sci. U.S.A.* **112**, 8708–8713 (2015).
26. L. Tian *et al.*, p85α recruitment by the CD300f phosphatidylserine receptor mediates apoptotic cell clearance required for autoimmunity suppression. *Nat. Commun.* **5**, 3146 (2014).
27. T. Matsukawa *et al.*, Ceramide-CD300f binding suppresses experimental colitis by inhibiting ATP-mediated mast cell activation. *Gut* **65**, 777–787 (2016).

28. J. S. Danik *et al*., Novel loci, including those related to crohn disease, psoriasis, and inflammation, identified in a genome-wide association study of fibrinogen in 17 686 women: The women's genome health study. *Circ. Cardiovasc. Genet.* **2**, 134–141 (2009).
29. M. Ban *et al*., A non-synonymous SNP within membrane metalloendopeptidase-like 1 (MMEL1) is associated with multiple sclerosis. *Genes Immun.* **11**, 660–664 (2010).
30. H. Xi *et al*., Negative regulation of autoimmune demyelination by the inhibitory receptor CLM-1. *J. Exp. Med.* **207**, 7–16 (2010).
31. A. F. Lloyd *et al*., Central nervous system regeneration is driven by microglia necroptosis and repopulation. *Nat. Neurosci.* **22**, 1046–1052 (2019).
32. M. L. Bennett *et al*., New tools for studying microglia in the mouse and human CNS. *Proc. Natl. Acad. Sci. U.S.A.* **113**, E1738–E1746 (2016).
33. A. Torres-Espín, J. Hernández, X. Navarro, Gene expression changes in the injured spinal cord following transplantation of mesenchymal stem cells or olfactory ensheathing cells. *PLoS One* **8**, e76141 (2013).
34. C. Ising *et al*., NLRP3 inflammasome activation drives tau pathology. *Nature* **575**, 669–673 (2019).
35. L. Tian *et al*., Enhanced efferocytosis by dendritic cells underlies memory T-cell expansion and susceptibility to autoimmune disease in CD300f-deficient mice. *Cell Death Differ.* **23**, 1086–1096 (2016).
36. F. N. Kaufmann *et al*., NLRP3 inflammasome-driven pathways in depression: Clinical and preclinical findings. *Brain Behav. Immun.* **64**, 367–383 (2017).
37. H. M. Kamens, T. J. Phillips, S. E. Holstein, J. C. Crabbe, Characterization of the parallel rod floor apparatus to test motor incoordination in mice. *Genes Brain Behav.* **4**, 253–266 (2005).
38. H. Peluffo *et al*., Overexpression of the immunoreceptor CD300f has a neuroprotective role in a model of acute brain injury. *Brain Pathol.* **22**, 318–328 (2012).
39. A. Ejarque-Ortiz *et al*., The receptor CMRF35-like molecule-1 (CLM-1) enhances the production of LPS-induced pro-inflammatory mediators during microglial activation. *PLoS One* **10**, e0123928 (2015).
40. Y. Zhang *et al*., An RNA-sequencing transcriptome and splicing database of glia, neurons, and vascular cells of the cerebral cortex. *J. Neurosci.* **34**, 11929–11947 (2014).
41. B. Kadriu *et al*., Acute ketamine administration corrects abnormal inflammatory bone markers in major depressive disorder. *Mol. Psychiatry* **23**, 1626–1631 (2018).
42. R. M. Hoek *et al*., Down-regulation of the macrophage lineage through interaction with OX2 (CD200). *Science* **290**, 1768–1771 (2000).
43. M. J. Gandal *et al*., Shared molecular neuropathology across major psychiatric disorders parallels polygenic overlap. **697**, 693–697 (2018).
44. A. Zeisel *et al*., Brain structure. Cell types in the mouse cortex and hippocampus revealed by single-cell RNA-seq. *Science* **347**, 1138–1142 (2015).
45. L. A. J. O'Neill, E. J. Pearce, Immunometabolism governs dendritic cell and macrophage function. *J. Exp. Med.* **213**, 15–23 (2016).
46. M. Liu *et al*., Metabolic rewiring of macrophages by CpG potentiates clearance of cancer cells and overcomes tumor-expressed CD47-mediated 'don't-eat-me' signal. *Nat. Immunol.* **20**, 265–275 (2019).
47. B. Stevens *et al*., The classical complement cascade mediates CNS synapse elimination. *Cell* **131**, 1164–1178 (2007).
48. N. R. Wilson *et al*., Presynaptic regulation of quantal size by the vesicular glutamate transporter VGLUT1. *J. Neurosci.* **25**, 6221–6234 (2005).
49. K. Nakayama, K. Kiyosue, T. Taguchi, Diminished neuronal activity increases neuron-neuron connectivity underlying silent synapse formation and the rapid conversion of silent to functional synapses. *J. Neurosci.* **25**, 4040–4051 (2005).
50. P. Willner, J. Scheel-Krüger, C. Belzung, The neurobiology of depression and antidepressant action. *Neurosci. Biobehav. Rev.* **37**, 2331–2371 (2013).
51. R. Dantzer, J. C. O'Connor, G. G. Freund, R. W. Johnson, K. W. Kelley, From inflammation to sickness and depression: When the immune system subjugates the brain. *Nat. Rev. Neurosci.* **9**, 46–56 (2008).
52. P. P. Katz, E. H. Yelin, Prevalence and correlates of depressive symptoms among persons with rheumatoid arthritis. *J. Rheumatol.* **20**, 790–796 (1993).
53. L. Capuron, A. Ravaud, R. Dantzer, Early depressive symptoms in cancer patients receiving interleukin 2 and/or interferon alfa-2b therapy. *J. Clin. Oncol.* **18**, 2143–2151 (2000).
54. A. Deczkowska *et al*., Disease-associated microglia: A universal immune sensor of neurodegeneration. *Cell* **173**, 1073–1081 (2018).
55. T. Franklin *et al*., Depression and sterile inflammation: Essential role of danger associated molecular patterns. *Brain Behav. Immun.* **72**, 2–13 (2018).
56. T. P. Schnieder *et al*., Microglia of prefrontal white matter in suicide. *J. Neuropathol. Exp. Neurol.* **73**, 880–890 (2014).
57. S. G. Torres-Platas, C. Cruceanu, G. G. Chen, G. Turecki, N. Mechawar, Evidence for increased microglial priming and macrophage recruitment in the dorsal anterior cingulate white matter of depressed suicides. *Brain Behav. Immun.* **42**, 50–59 (2014).
58. M. L. Estes, A. K. Mcallister, Alterations in immune cells and mediators in the brain: It's not always neuroinflammation! *Brain Pathol.* **24**, 623–630 (2014).
59. World Health Organization, "Depression and other common mental disorders: Global health estimates" (World Health Organization,Geneva, 2017).
60. I. Mahar, F. R. Bambico, N. Mechawar, J. N. Nobrega, Stress, serotonin, and hippocampal neurogenesis in relation to depression and antidepressant effects. *Neurosci. Biobehav. Rev.* **38**, 173–192 (2014).
61. C. Moret, M. Briley, The importance of norepinephrine in depression. *Neuropsychiatr. Dis. Treat.* **7** (suppl. 1), 9–13 (2011).
62. F. Filipello *et al*., The microglial innate immune receptor TREM2 is required for synapse elimination and normal brain connectivity. *Immunity* **48**, 979–991.e8 (2018).
63. B. A. Györffy *et al*., Local apoptotic-like mechanisms underlie complement- mediated synaptic pruning. *Proc. Natl. Acad. Sci. U.S.A.* **115**, 6303–6308 (2018).
64. W. Chung *et al*., Novel allele-dependent role for APOE in controlling the rate of synapse pruning by astrocytes. *Proc. Natl. Acad. Sci. U.S.A.* **113**, 10186–10191 (2016).
65. P. F. Renshaw *et al*., Multinuclear magnetic resonance spectroscopy studies of brain purines in major depression. *Am. J. Psychiatry* **158**, 2048–2055 (2001).
66. P. J. Allen, K. E. D. Anci, R. B. Kanarek, P. F. Renshaw, Chronic creatine supplementation alters depression-like behavior in rodents in a sex-dependent manner. *Neuropsychopharmacology* **35**, 534–546 (2010).
67. I. K. Lyoo *et al*., A randomized, double-blind placebo-controlled trial of oral creatine monohydrate augmentation for enhanced response to a selective serotonin reuptake inhibitor in women with major depressive disorder. *Am. J. Psychiatry* **169**, 937–945 (2012).
68. J. K. Götzl *et al*., Opposite microglial activation stages upon loss of PGRN or TREM 2 result in reduced cerebral glucose metabolism. *EMBO Mol. Med.* **11**, e9711 (2019).
69. H. Hirbec *et al*., The microglial reaction signature revealed by RNAseq from individual mice. *Glia* **66**, 971–986 (2018).
70. S. De, *et al*., Two distinct ontogenies confer heterogeneity to mouse brain microglia. *Development* **145**, dev152306 (2018).
71. O. Matcovitch-Natan *et al*., Microglia development follows a stepwise program to regulate brain homeostasis. *Science* **353**, aad8670 (2016).
72. S. Picelli *et al*., Smart-seq2 for sensitive full-length transcriptome profiling in single cells. *Nat. Methods* **10**, 1096–1098 (2013).